Title
Sterol Structure Strongly Modulates Membrane–Islet Amyloid Polypeptide Interactions

Journal
Biochemistry, 57(12)

ISSN
0006-2960

Authors
Zhang, Xiaoxue
London, Erwin
Raleigh, Daniel P

Publication Date
2018-03-27

DOI
10.1021/acs.biochem.7b01190

Peer reviewed

HHS Public Access

Author manuscript

Biochemistry. Author manuscript; available in PMC 2019 March 27.

Published in final edited form as:

Biochemistry. 2018 March 27; 57(12): 1868–1879. doi:10.1021/acs.biochem.7b01190.

Sterol Structure Strongly Modulates Membrane-IAPP Interactions

Xiaoxue Zhang[1], **Erwin London**[1,2,*], and **Daniel P. Raleigh**[1,3,*]

[1]Department of Chemistry, Stony Brook University, Stony Brook, NY, 11794-3400

[2]Department of Biochemistry and Cell Biology, Stony Brook University, Stony Brook, NY, 11794-5215

[3]Graduate Program in Biochemistry and Structural Biology, Stony Brook University, Stony Brook, NY, 11794-5215

Abstract

Amyloid formation has been implicated in a wide range of human diseases, and the interaction of amyloidogenic proteins with membranes are believed to be important for many of these. In type-2 diabetes, human islet amyloid polypeptide (IAPP) forms amyloid which contributes to β-cell death and dysfunction in the disease. IAPP membrane interactions are potential mechanisms of cytotoxicity. *In vitro* studies have shown that cholesterol significantly modulates the ability of model membranes to induce IAPP amyloid formation and IAPP mediated membrane damage. It is not known if this is due to the general effects of cholesterol on membranes or because of specific sterol-IAPP interactions. The effects of replacing cholesterol with eight other sterols/steroids on IAPP binding to model membranes, membrane disruption and membrane mediated amyloid formation were examined. The primary effect of the sterols/steroids on the IAPP membrane interactions was found to reflect their effect upon membrane order, as judged by fluorescence anisotropy measurements. Specific IAPP sterols/steroids interactions have smaller effects. The fraction of vesicles which bind IAPP was inversely correlated with the sterols/steroids' effect on membrane order, as was the extent of IAPP induced membrane leakage and the time to form amyloid. The correlation between the fraction of vesicles binding IAPP and membrane leakage was particularly tight, suggesting the restriction of IAPP to a subset of vesicles is responsible for incomplete leakage.

Graphical Abstract

[*]**Corresponding Authors:** D.P.R: daniel.raleigh@stonybrook.edu, phone: (631) 632-9547; Fax: (631) 632-7960. E.L: erwin.london@stonybrook.edu, phone, (631) 632-8564.

Author Contributions

X.Z. designed and conducted experiments and analyzed data. D.P.R. and E.L. designed, directed and supervised the project. D.P.R., E.L. and X.Z. wrote the manuscript.

ASSOCIATED CONTENT

Supporting Information: Five figures showing the effect of different sterols on the time course of amyloid formation by hIAPP, the time course of hIAPP induced membrane damage, correlations between membrane order and leakage, peptide binding as a function of lipid concentration and TEM images. In addition one table containing data on effective diameters of LUVs and another table containing all values of T_{50} and leakage. This material is available free of charge on the ACS Publications website.

Notes

The authors declare no competing financial interest.

For Table of Contents Use Only

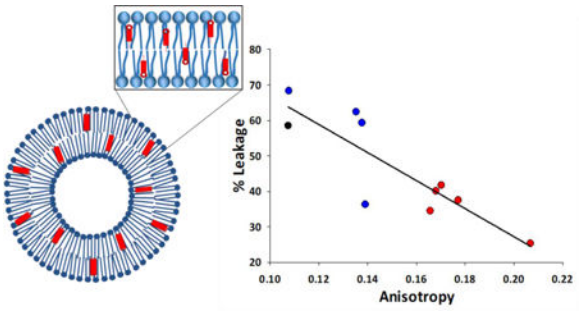

Keywords

Amyloid; Amylin; Islet Amyloid Polypeptide; Sterol; Membrane Order; Tight Lipid Packing; Peptide Membrane Interactions; Type-2 Diabetes

INTRODUCTION

Islet amyloid polypeptide (IAPP also known as amylin) is a 37 residue pancreatic hormone which is co-secreted with insulin from the β-cells in the islets of Langerhans[1]. IAPP plays a role in regulating glucose metabolism, but aggregates to form islet amyloid in type 2 diabetes (T2D) by unknown mechanisms[2–7]. The process of islet amyloid formation contributes to the loss of β-cell mass and β-cell death in T2D and also plays a key role in the failure of islet grafts[4, 5, 8–14].

The mechanisms of IAPP induced cell death are not completely understood, but membrane permeabilization has been proposed to play a role[13, 15–17]. A large body of biophysical work has investigated the interactions of IAPP with model membranes, usually in the form of large unilamellar vesicles (LUVs). Early studies focused on binary systems containing a zwitterionic lipid and an anionic lipid, usually phosphatidylserine[18–23]. Such vesicles enhance the rate of IAPP amyloid formation and IAPP efficiently induces leakage from them. More recent studies have highlighted the importance of cholesterol in modulating membrane-IAPP interactions[24–31]. Cholesterol is an important component of cellular membranes that significantly affects membrane properties, and is important for the uptake of hIAPP by cells *in vivo*[24, 29, 31–36]. It has been observed that cholesterol significantly inhibits phospholipid-catalyzed IAPP amyloid formation and reduces the ability of IAPP to induce model membrane leakage, but the molecular basis of these effects is not known[25, 26, 30, 31, 37].

Prior studies found that physical properties of membranes, such as membrane order, curvature and lipid composition, influence the binding of IAPP to membranes[38–41]. For example, it has been shown that in the presence of cholesterol IAPP inserts in a small number of larger protein clusters, i.e. clusters with a larger number of IAPP molecules[26]. It has also been shown that cholesterol can limit leakage from membranes[30, 37]. Because cholesterol has dramatic effects on the biophysical properties of membranes some workers have suggested that these are the cause of its effects on amyloidogenic protein-membrane

interactions[26, 28–30, 34, 39, 40, 42]. However, cholesterol can also interact directly with membrane-bound polypeptides and specific cholesterol-polypeptide interactions have been proposed to be important as well[27, 34, 43–46].

Here we systematically examine the effects of various sterols on the ability of LUVs to promote IAPP amyloid formation and on the ability of IAPP to disrupt model membranes (Figure 1).

The sterols were chosen to explore the potential importance of the OH group at carbon position 3, double bond presence and position, hydrocarbon tail structure, and the planarity of the sterol rings. No obvious correlation was observed with specific chemical features of the sterols. Instead the rate of amyloid formation and IAPP-induced membrane leakage was strongly correlated with the effect of sterols on membrane packing as judged by fluorescence anisotropy measurements. Sterols which led to more tightly packed lipids in membranes resulted in slower amyloid formation and decreased membrane leakage. The decrease in leakage appears to be a consequence of a sterol-induced restriction in the fraction of vesicles that bind IAPP.

MATERIALS AND METHODS

Materials.

1,2-dioleoyl-sn-glycero-3-phosphoethanolamine-N-(7-nitro-2–1,3-benzoxadiazol-4-yl) (NBD-DOPE), 1-palmitoyl-2-oleoyl-sn-glycero-3-phosphocholine (POPC), 1-palmitoyl-2-oleoyl-sn-glycero-3-phospho-L-serine (sodium salt) (POPS), and cholesterol were obtained from Avanti Polar Lipids. 5α-cholestan-3-one, cholestenone, coprostanol, and epicholesterol were obtained from Steraloids. 5(6)-carboxyfluorescein, 7-dehydrocholesterol, cholestanol, dimethyl sulfoxide (DMSO), ergosta-5,7,9(11),22-tetraen-3β-ol (DHE), hexafluoroisopropanol (HFIP), lathosterol, pregnenolone, thioflavin-T, triton X-100 and sucrose were obtained from Sigma-Aldrich. The concentrations of unlabeled lipids were determined by dry weight and that of NBD-DOPE lipids by absorbance using $\varepsilon_{\text{NBD-DOPE}}$ = 21, 000 M^{-1} cm^{-1} at 460 nm in methanol. Sterol purity were assayed by TLC and no significant impurities were detected.

Peptide Synthesis and Purification.

Human islet amyloid polypeptide was synthesized on a 0.1 mmol scale using 9-fluoronylmethoxycarbonyl (Fmoc) chemistry with a CEM microwave peptide synthesizer. The 5-(4'-fmoc-aminomethyl-3', 5-dimethoxyphenol) valeric acid (Fmoc-Pal-PEG-PS) resin was used to provide an amidated C-terminus. Fmoc-protected pseudoproline dipeptide derivatives were incorporated at positions 9–10, 19–20 and 27–28[47]. Double coupling were performed for all pseudoprolines, Arg and β-branched residues. A maximal temperature of 50 °C was used for the His and Cys coupling to reduce racemization[48]. Standard trifluoroacetic acid (TFA) methods were used to cleave peptides from the resin. The crude peptides were dissolved in 20% acetic acid (vol/vol) to increase solubility and lyophilized. The disulfide bond was formed by dissolving dry peptide in pure DMSO at room temperature[49]. The peptide was purified by reverse-phase high-performance liquid

chromatography with a Proto 300 C18 preparative column (10 mm x 250 mm). A two-buffer system was used: buffer A consisted of 100% H_2O and 0.045% HCl (vol/vol), buffer B consisted of 80% acetonitrile, 20% H_2O and 0.045% HCl (vol/vol). HCl was used as the ion-pairing agent instead of TFA, as TFA can impact amyloid formation and affect cell toxicity assays[50]. The molecular weight of the pure product was confirmed using a Bruker AutoFlexII MALDI-TOF/TOF mass spectrometer: human IAPP, expected 3903.3, observed 3903.8. Analytical HPLC was used to check peptide purity before experiments. The purity is estimated to be 98% or higher based on HPLC. A single peak was detected by analytical reverse phase HPLA with a C18 column. This is an important control because IAPP can deamidate and this can affect IAPP amyloid formation[51, 52].

Preparation of Peptide Samples.

Material from the same synthesis was used in all biophysical studies to ensure comparable conditions for all experiments. Peptide stock solutions were prepared by dissolving pure peptide in 100% HFIP at a concentration of 0.8 mM, filtering through a 0.22 μM Millex low protein binding durapore membrane filter to remove preformed aggregates, and stored at 4 °C. Aliquots were lyophilized for 20–24 hours to remove organic solvent and redissolved in buffer at the desired concentration immediately before the experiments started. The peptide concentration was measured by absorbance at 280nm using $\varepsilon = 1600\ M^{-1}cm^{-1}$.

Preparation of Large Unilamellar Vesicles.

Large unilamellar vesicles (LUVs) were prepared from multilamellar vesicles (MLV). MLVs were prepared by dissolving lipids in chloroform at the desired concentration in a glass tube. Mixtures were evaporated with nitrogen gas and were dried in high vacuum for at least 1 h to completely remove the residual organic solvent. The resulting lipid mixtures were then dispersed in tris buffer (20 mM Tris·HCl, 100 mM NaCl at pH 7.4) and agitated at 55 °C for at least 30 min. Samples were cooled to room temperature before use. LUVs were prepared by subjecting the MLVs to 8 freeze-thaw cycles and then passing through a 100 nm polycarbonate filter (Avanti Polar Lipids) 15 times to obtain uniform vesicle size. The phospholipid concentration was determined by the method of Stewart[53]. For the membrane leakage experiments, LUVs containing 5(6)-carboxyfluorescein were prepared using the same protocol except that 5(6)-carboxyfluorescein was dissolved in tris buffer at a concentration of 80 mM before lipid hydration. Nonencapsulated 5(6)-carboxyfluorescein was removed from 5(6)-carboxyfluorescein-filled LUVs using a PD-10 desalting column (GE Healthcare Life Sciences) and elution with tris buffer. Dynamic light scattering (DLS) was used to check the effective diameter and polydispersity of each vesicle preparation before use. A fresh vesicle solution was used for each experiment.

Dynamic Light Scattering.

Dynamic light scattering experiments were performed on a NanoBrook 90Plus Particle Size Analyzer with a 35 mW red diode laser. The wavelength of irradiation was 640 nm. Membrane samples were prepared to a final concentration of 40 μM with tris buffer. For each sample, three runs were taken at 25 °C with 60 seconds per run. The average diameter (effective diameter) and the distribution width (polydispersity) were calculated using the 90Plus Particle Sizing Software.

Anisotropy Measurements.

Anisotropy measurements were conducted at room temperature using a SPEX automated Glan-Thompson polarizer accessory. Anisotropy values were calculated from the fluorescence intensities with polarizing filters set at all combinations of horizontal and vertical orientations. Fluorescence intensity in background samples lacking fluorophore were subtracted. Anisotropy (A) was calculated from the equation

$$A=[((Ivv\times Ihh)(Ivh\times Ihv))-1][((Ivv\times Ihh)(Ivh\times Ihv))+2], \quad (1)$$

where Ivv, Ihh, Ihv, and Ivh are the various fluorescence intensities after subtraction of background intensities with the excitation and emission polarization filters, respectively, in vertical (v) and horizontal (h) orientations.

Sucrose Density Gradient Centrifugation Assays.

Sucrose gradient centrifugation was performed using a Beckman L8–55M ultracentrifuge with an SW-60 rotor. Sucrose gradients were prepared by freezing 3.5 ml of 10% (w/w) sucrose at –20 °C in centrifuge tubes overnight and thawing to room temperature. Sucrose concentrations in the fractions were estimated using a refractometer. The highest density was 20 percent sucrose (bottom layer) and the lowest was 5 percent sucrose (top layer). Vesicles contained 2 mole percent NBD-DOPE to allow visualization. Vesicles were incubated with hIAPP until amyloid formation was complete. 500 μl samples were loaded on top of the gradients and samples were then centrifuged for 45 minutes at 37,500 rpm (190,000 G). Vesicles that bind substantial peptide migrate to the bottom layer of the gradient while those that do not float on top of the gradient. The two lipid-containing layers were removed and diluted to 1.2 ml with tris buffer. The amount of NBD-DOPE in each layer was quantified using a SPEX FluoroLog 3 spectrofluorometer with excitation and emission wavelengths of 465 nm and 534 nm. The slit bandwidths for fluorescence measurements were set to 4.0 nm for both excitation and emission. Background intensities in samples lacking fluorescent probe were negligible (1–2%), and were generally not subtracted from the reported values.

Thioflavin-T Fluorescence Assays.

Thioflavin-T fluorescence experiments were performed using a Beckman Coulter DTX880 plate reader with excitation and emission wavelengths of 430 nm and 485 nm, respectively. Samples were incubated in 96-well quartz microplate at 25 °C. Samples contained 20 μM peptide in tris buffer with 32 μM Thioflavin-T. This concentration of IAPP was chosen to yield a peptide to lipid ratio of 1:20 since this is typical of values used for studies of hIAPP-membrane interactions[22, 37, 54, 55]. Experiments in the presence of membranes were initiated by adding LUVs at a 400 μM lipid concentration. Uncertainties in T_{50} were estimated by conducting measurements in triplicate using different solutions of hIAPP.

Membrane Permeability Assays.

Leakage experiments were performed using a Beckman Coulter DTX880 plate reader with excitation and emission wavelength filters of 485 nm and 535 nm, respectively. All of the samples were incubated in 96-well quartz microplate at 25 °C. 400 μM lipid LUVs with

encapsulated 5(6)-carboxyfluorescein were used. Peptide concentration was 20 μM. The fluorescence signal of the 5(6)-carboxyfluorescein, which increases upon leakage out of vesicles, was continuously measured during the course of each experiment. The maximum leakage for totally disrupted membranes was measured by adding the detergent Triton X-100 to a final concentration of 0.2% (vol/vol).

The percent change in 5(6)-carboxyfluorescein fluorescence was calculated as:

$$\text{Percent Fluorescence Change} = 100\% \times \left[F(T) - F_{baseline}\right] / \left(F_{max} - F_{baseline}\right) \quad (2)$$

Where F(T) is the fluorescence intensity at time T, F_{max} is the fluorescence intensity when all of the vesicles have been disrupted with Triton X-100 and $F_{baseline}$ is the fluorescence intensity before addition of hIAPP. The percent change in fluorescence will equal the percentage change in leakage provided the 5(6)-carboxyfluorescein fluorescence response is linear. Previous work has shown that this is a reasonable assumption for the condition used in studies[37]. Uncertainties were estimated by repeating the measurements three times using different stock solutions of hIAPP.

Transmission Electron Microscopy.

TEM was performed at the Life Science Microscopy Center at Stony Brook University. Aliquots of samples from the thioflavin-T fluorescence experiments were used to prepare TEM samples. Eight microliters of the solution were blotted on a carbon-coated Formvar 300 mesh copper grid for 1 min and then negatively stained for additional 1 min with saturated uranyl acetate.

Förster Resonance Energy Transfer (FRET) Measurements of Peptide Binding.

A donor/acceptor pair of tyrosine (in hIAPP)/ DHE was used. Fluorescence was measured using an Applied Phototechnology fluorescence spectrophotometer with an excitation wavelength of 270 nm and an emission wavelength of 305 nm. F samples contained a hIAPP/vesicle with a mixture of unlabeled lipid and 2 mol% DHE, while Fo samples contained a hIAPP/vesicle with a mixture of unlabeled lipid and 2 mol% cholesterol in place of DHE. Background for F samples contained unlabeled lipid with DHE without peptide. Background samples for Fo contained pure unlabeled lipid without peptide. For FRET experiments, LUVs were injected into 20 μM hIAPP/tris buffer at concentrations ranging from 0 to 960 μM lipid. Backgrounds were LUVs injected into tris buffer.

RESULTS

The primary sequence of hIAPP and the structure of the sterols studied are displayed in Figure-1. The polypeptide contains an amidated C-terminus and a disulfide bond between residue 2 and 7. Positively charged residues include Lys-1, Arg-11 and potentially His-18 depending upon its pKa. To analyze the effect of sterol structures upon membrane IAPP interactions, nine sterols were chosen. They can be broadly classified in terms of properties including the ability or inability to support tight lipid packing (see below). Comparison of

the effects of the different sterols allows specific features in the sterol structure to be probed, including a) the presence or absence of a hydroxyl group in position 3, b) hydroxyl group stereochemistry, c) the presence or absence of a double bond between the 4 and 5 carbons in the sterol A ring, or between 5 and 6 carbons or 7 and 8 carbons in the sterol B ring, d) the presence and absence of a normal aliphatic tail and f) the planarity of the sterol rings (Figure-1). Note that the cholesterol analogues without a hydroxyl group are formally speaking steroids not sterols, but we will refer to all of the cholesterol analogs as sterols for simplicity.

Analysis of the ability of sterols to support tight lipid packing.

First, the ability of the sterols to support tight lipid packing was analyzed. These experiments were carried out using LUVs containing POPC, POPS and various sterols at 25°C, by measuring the fluorescence anisotropy of DPH incorporated into the lipid mixtures. The degree of DPH fluorescence anisotropy/polarization reflects the degree to which a DPH molecule reorients while in the excited state. This degree of reorientation decreases (anisotropy increases) in an environment where motion is restricted such as a tight packing/liquid ordered state-promoting environment[56]. Table-1 lists the effects of various sterols on DPH anisotropy. Sterols were chosen based on their reported ability to promote or inhibit liquid ordered state formation[32, 57–59]. In general terms, sterols that promote the formation of ordered lipid domains should also promote tight lipid packing in model membranes. The anisotropy values observed were consistent with this hypothesis. At 25°C, the values of the anisotropy for POPC/POPS mixed vesicles ranged from 0.107 to 0.112, depending on the percentage of POPS. Although POPS/POPC vesicles are not likely to form ordered domains without sterols, sterols that promote ordered domain formation (sterols 2–6 [32, 57–59]) showed the largest effect on tight lipid packing, with anisotropy values in the range 0.166 to 0.236 in mixed vesicles containing 20 mol% sterols and 80 mol% POPC/POPS, while sterols that do not promote ordered domain formation (sterols 7–10 [32, 57, 58]) had a smaller effect upon packing, with anisotropy values in the range 0.111 to 0.157 under the same conditions. Addition of 10 mol% POPS into mixed vesicles did not change the anisotropy values significantly, but increasing the sterol mol% from 20 mol% to 40 mol% increased anisotropy values; with a range of 0.199 to 0.230 for raft promoting sterols and 0.119 to 0.172 for sterols that do not support raft formation. Overall, sterols that promote ordered domain formation give higher values of anisotropy in mixed LUVs than values for sterols that do not promote ordered domain formation, confirming that the former promote tight lipid packing more strongly than the latter.

The effect of sterols on the ability of vesicles to bind peptide: An inverse correlation between membrane order and the fraction of vesicles that bound peptide.

In our previous studies of IAPP interactions with model vesicles, we found that a subset of the LUVs bind peptide and another subset either do not, or bind only a very small number of peptides[37]. To test if the sterols affect the ability of LUVs to bind peptide, we conducted sucrose gradient experiments using mixed LUVs containing POPC with POPS and different sterols. We choose a lipid to peptide ratio of 20:1 and a hIAPP concentration of 20 μM for these and all following studies since this is typical of values used for biophysical studies of membrane catalyzed hIAPP amyloid formation. The LUVs were labeled with 2 mol% of the

fluorescence lipid probe NBD-DOPE. After incubation with peptide, the LUVs were centrifuged in a 5 to 20 percent sucrose gradient. Two fractions were observed in the presence of hIAPP, a lighter fraction which floats at the top of the gradient in the same position observed for control LUVs in the absence of peptide, and a second fraction which pellets. Because vesicle with bound peptide are more dense, the lighter fraction contains vesicles with little hIAPP bound while the pellet contains those which bind a high amount of peptide. The fact that there were two fractions indicated that not all vesicles bound much peptide under the conditions examined. Table-2 lists the fraction of vesicles that bind peptide for mixed vesicles containing POPC, POPS and various sterols. A larger percentage of POPS containing vesicles bound peptide compared with vesicles that did not contain POPS. The fraction of sterols also had a large effect on the fraction of vesicles that bind peptide.

There is a statistically significant inverse correlation between the fraction of vesicles that bind peptide and the effect of different sterols on membrane order (Figure-2). A larger fraction of the LUVs that contain sterols which do not promote very tight lipid packing bound peptide than did LUVs which contained sterols that strongly promote tight packing. This is true for all composition sets with varying fractions of POPS and sterols. The square of the correlation coefficient, R^2, varied with the presence of POPS and sterol concentration over the range of 0.6637 to 0.7719. This statistically significant, but imperfect correlation suggests that other factors also influence the fraction of vesicles that bind peptide (see Discussion).

The differences in the percent of vesicles which bound peptide might reflect lipid and sterol composition-dependent differences in how much peptide was bound to the vesicles. To test this hypothesis, a control experiment using FRET measurements was performed to measure the amount of peptide bound to LUVs under our experimental conditions. A donor−acceptor pair of tyrosine (in hIAPP) and ergosta-5,7,9(11),22-tetraen-3β-ol (DHE) was used. LUVs containing 2 mol% DHE or with 2 mol% cholesterol in place of DHE were injected into 20 μM hIAPP at LUV concentrations ranging from 0 to 960 μM. Binding of both hIAPP freshly dissolved in aqueous solution and samples pre-incubated to form hIAPP fibrils were tested separately. Binding of IAPP with LUVs leads to energy transfer from donor tyrosine to acceptor DHE, resulting in a decrease of tyrosine fluorescence. Tyrosine fluorescence was recorded during the titration. Data were collected for POPS-only LUVs, POPC-only LUVs, and LUVs containing 80 mol% POPC with 20 mol% cholesterol (promotes tight lipid packing) and LUVs containing 80 mol% POPC with 20 mol% pregnenolone (does not promote tight lipid packing). Binding of peptide to POPS-only vesicles exhibited saturation at lower lipid concentrations and a slightly larger level of FRET (lower F/Fo) than the other samples. There were only small differences between POPC-only vesicles and POPC with 20 mol% sterol vesicles, with slightly weaker binding to vesicles with cholesterol, as indicated by a higher lipid concentration for half-maximal FRET (Figure-S1). More importantly, the experiments revealed that peptide binding was saturated by excess lipid under our experimental conditions of 20 μM peptide with 400 μM lipid for all conditions. Thus, the centrifugation studies described above are not explained by significant differences in the amount of vesicle-bound peptide.

hIAPP is more effective at permeabilizing LUVs which contain sterols that do not strongly promote tight lipid packing.

We next examined the effects of different sterols on membrane leakage using mixed binary LUVs with POPC as the zwitterionic lipid. Membrane leakage was followed using fluorescence-detected 5(6)-carboxyfluorescein leakage assays. 5(6)-carboxyfluorescein is a highly fluorescent molecule whose fluorescence is self-quenched at high concentrations. High concentrations of the dye are encapsulated into LUVs, and upon membrane disruption/pore formation by hIAPP, the dye is released and the consequent dilution leads to relief of self-quenching and thus enhanced fluorescence. The percent fluorescence change of the dye is related to the percent membrane leakage.

We measured the time course of leakage of mixed LUVs during incubation with hIAPP over times long enough to form amyloid. Inclusion of sterols that promote very tight lipid packing decreased the fluorescence change relative to the change observed with pure POPC vesicles, indicating decreased leakage, while inclusion of sterols that do not strongly promote tight lipid packing in vesicles did not have significant effects on membrane leakage (Figure-3, Figure-S2, Table-S2). Significant leakage was detected for incubation times noticeably less than the time required to from amyloid, indicating that leakage can induced by oligomeric species formed early in the amyloid self-assembly process.

Dye leakage was also measured for vesicles that contained 10 mol% POPS and with vesicles in which the sterol percentage was increased from 20 to 40 mol%. Adding 10 mol% of anionic lipids led to a significant increase in membrane leakage for both short and long incubation times for all sterols tested. Increasing the concentration of sterols that strongly promote tight lipid packing from 20 to 40 mol% significant decreased membrane leakage, while changing the percentage of sterols that do not strongly promote tight lipid packing did not have significant effects upon leakage (Figure-S2, Table-S2).

The amount of leakage observed after incubation for a time long enough to ensure amyloid formation has an extremely strong correlation (R^2 = 0.9700–0.9941) with the fraction of vesicles pelleted, i.e. those vesicles which bound peptide (Figure-4). This indicates that the extent of leakage reflects the fraction of vesicles that bind substantial amounts of peptide. It also suggests there is little or no leakage from the vesicles that do not bind substantial amounts of peptide, and explains why the observed percentage leakage for some lipid compositions remains at a low level and does not reach 100% even for long incubation times, and even though hIAPP is added in excess in these experiments.

Sterols that promote tight lipid packing have an inhibitory effect on amyloid formation.

We next examined the effects of different sterols on hIAPP amyloid formation using mixed binary or ternary LUVs that contained 80 mol% POPC and 20 mol% sterols. Amyloid formation was monitored by fluorescence thioflavin-T assays. Thioflavin-T is a small fluorophore whose quantum yield is low in solution, but is enhanced upon binding to amyloid fibrils. Thioflavin-T assays are a well-documented approach to follow hIAPP amyloid in solution and in the presence of membranes. Transmission electron microscopy (TEM) was used to visualize the final products of the amyloid formation assays to provide

an independent test of amyloid formation. This is an important control since thioflavin-T is an extrinsic probe and sometimes gives a low signal even in the presence of amyloid fibrils[60]. Under the conditions of our study, in the absence of membranes, hIAPP has a T_{50}, defined as the time to reach 50 percent of the signal change due to amyloid formation in a thioflavin-T amyloid assay, of 25.8 hours in 20 mM tris buffer (Table-S2). We first examined LUVs that did not contain POPS. The rate of hIAPP amyloid formation, as judged by T_{50} values, was inhibited in the presence of vesicles containing sterols that promote tight lipid packing, with T_{50} values increasing from 27.6 hours to 48.2 hours, when compared to the rate of amyloid formation in the presence of POPC vesicles (19.8 hours). The rate of hIAPP amyloid formation in the presence of vesicles containing sterols that do not promote very tight lipid packing was similar to that observed for LUVs without sterol, with T_{50} values from 18.5 hours to 20.2 hours. Coprostanol was an exception, with a T_{50} values of 38.4 hours, even though it is a sterol that does not promote very tight lipid packing (Figure-5, Table-S2). T_{50} values which differ by 2 or more hours are judged to be significant. TEM was used to probe the morphology of the amyloid fibrils which result from these experiments and the morphology of the vesicles. No detectable change in fibril morphology as a function of vesicle composition was observed at the level detectable by TEM (Figure-S5).

We next examined the effects of adding 10 mol% POPS as well as increasing the sterol percentage from 20 mol% to 40 mol%. POPS accelerated the rate of amyloid formation in all cases, as judged by the T_{50} values (Figure-S4, Table-S2), while increasing the sterol fraction led to slower rates of amyloid formation. This effect was more significant in vesicles containing sterols that promote very tight lipid packing. For example with cholesterol the T_{50} value decreased from 29.1 hours to 11.4 hours upon inclusion of 10 mol % POPS, and then increased to 17.4 hours when the cholesterol percentage was increased from 20 mol% to 40 mol% while maintaining the POPS faction at 10 mol%. Vesicles containing sterols that do not promote very tight lipid packing also showed a decrease in T_{50} when POPS was added. A small increase in T_{50} for vesicles containing POPS was observed when the concentrations of these sterols were increased. For example, T_{50} values changed from 20.2 hours to 8.8 hours for vesicles containing 5α-cholestan-3-one upon addition of POPS. A modest change to T_{50} = 9.5 hours was observed when the sterol concentration was increased from 20 mol% to 40 mol% while maintaining the POPS concentration.

As noted above, sterols that strongly promote tight lipid packing had an inhibitory effect on amyloid formation, but those that only weakly promote tight lipid packing had a much smaller inhibitory effect on amyloid formation, or even accelerated amyloid formation a bit.

Overall, a significant correlation (R^2 = 0.6125–0.8117) was observed between the time required to form amyloid and the effect of different sterols on membrane order, as judged by anisotropy values (Figure-6). This statistically significant, but imperfect correlation suggests that other factors also influence the fraction of vesicles that bind peptide (see Discussion).

There is also a significant inverse correlation between the time required to form amyloid and the fraction of vesicles that bind peptide (Figure-7). However, the correlation (R^2 ranging from 0.6347 to 0.8161), while strong, is not perfect, indicating that the effect of sterol

structure on the fraction of vesicles that bind peptide does not fully explain the differences in amyloid formation (see Discussion).

DISCUSSION:

Prior studies have explored several aspects of the effect of cholesterol on IAPP interactions with membranes[25–31, 39, 40], but have not investigated the extent to which the effects of cholesterol were due to its effect on membrane physical properties or direct/specific interactions with IAPP.

Other studies have examined the behavior of IAPP in cholesterol-containing membranes that have co-existing ordered and disordered domains (Ld)[30, 61]. It has been reported that IAPP localizes primarily in Ld domains and that membranes with domains accelerate IAPP induced membrane leakage and fiber growth[30]. In such case, cholesterol has been reported to enhance fiber growth. It should be noted that protein behavior can differ in membranes lacking domains from that in domain-containing membranes because interactions between protein and lipid can be enhanced at the boundary between ordered and disordered domains[62–64], and because the interaction of protein and lipid can influence the properties of domains and thus the properties at domain boundaries[30, 65].

The data presented in this study indicate that sterols modulate IAPP-membrane interactions in the vesicles tested mainly by affecting the tightness of lipid packing, rather than directly interactions involving specific chemical features of sterol. Sterols which led to more tightly packed membrane lipids generally resulted in binding of IAPP to a smaller fraction of vesicles, decreased membrane leakage, and slowed amyloid formation. Sterols that did not lead to tighter packing generally had relatively little effect upon IAPP-membrane interaction.

The correlation between the fraction of vesicles that bind peptide and vesicle leakage was revealed in this study to be extremely strong, and indicates that it is the subpopulation of vesicles that bind substantial amounts of peptide that undergo leakage. This implies that the inhibition of leakage by sterols that increase membrane order reflects the influence of those sterols on the distribution of IAPP in the vesicles. This likely reflects the clustering of IAPP into a lesser number of (larger) clusters in cholesterol-containing membranes[26]. An alternative explanation for the effect of sterol on leakage could involve a sterol-dependent effect on the amount of bound peptide, but this is ruled out by the observation that the vast majority of peptides were vesicle bound with and without sterol under our experimental conditions. It should also be noted that the slope of a plot of the fraction of vesicles that bind peptide vs membrane leakage (Figure-4) was <1.0 (~ 0.85). The deviation of the slope from one could result from a small fraction of vesicles that bind peptide, but do not form pores, or from slight non-linearity of the carboxyfluorescein leakage assay[37]. Why cholesterol and sterols that promote tight lipid packing promote IAPP-IAPP interactions leading to fewer, but larger clusters is not obvious. One possibility is that tight lipid packing might inhibit/slow IAPP binding to the lipid bilayer and allow IAPP to oligomerize in solution. This could result in larger portion of the IAPP binding to vesicles as oligomers which, in turn, could

lead to a higher level of positive cooperativity if oligomers bound to a vesicle are especially effective in nucleating additional peptide binding to that vesicle.

The possibility that cholesterol and other sterols that promote tight lipid packing may result in more highly cooperative binding with IAPP molecules forming larger clusters in a smaller number of vesicles may also help rationalize why cholesterol can inhibit amyloid formation. If IAPP molecules are tightly bound to each other, they may be stably trapped in a membrane bound oligomeric state which would act as a pre-fibrillar thermodynamic sink.

There were also some deviations from a strict linear correlation between tightness of lipid packing induced by sterols and the various membrane-hIAPP interactions. These likely result from secondary effects reflecting the different chemical features of the different sterols, for example, differences in the ability to form hydrogen bonds between IAPP polar residues and the sterol hydroxyl group, or differences in van der Waals interactions between sterol rings, methyl and/or iso-octyl groups and the hydrophobic and aromatic amino acid residues in IAPP. The observed effects might also involve the way that the sterols interact with other lipids, for example by an effect on overall lipid curvature that somehow alters interactions with IAPP. Perhaps the most striking example of deviation from the observed correlation of lipid packing and membrane binding was that of coprostanol, for which there was a decreased fraction of vesicles binding hIAPP and a decrease in hIAPP-induced leakage relative to vesicles without sterol, even though coprostanol did not promote tight lipid packing. Interestingly, the effect of coprostanol on amyloid formation did not differ greatly from those induced by sterols that did not promote tight lipid packing in vesicles containing POPS, suggesting that IAPP clusters in coprostanol-containing vesicles are not conformationally trapped in the same manner as they are in vesicles that promote tight lipid packing.

To summarize, this work presents a systematic study of the effect of varying sterol structure on IAPP membrane interactions. Future studies could examine the conformation of bound IAPP using spectroscopy methods. Previous studies have exclusively made use of cholesterol and it was not possible to determine to what extent cholesterol exerts its effects by modulating the biophysical properties of membranes as opposed to specific sterol interactions. We have shown that the primary effect of different sterols on IAPP amyloid formation and IAPP induced membrane leakage (via its effect upon the fraction of vesicles that bind peptide) is due to the effect of the sterols upon lipid packing. Effects due to specific sterol IAPP interactions are less pronounced, although they may influence some IAPP-membrane interactions. The approach illustrated here is not limited to IAPP and can be applied to other amyloidogenic proteins. Along these lines, cholesterol is known to modulate Aβ membrane interactions, but a detailed molecular level understanding of the effects is lacking[66–70].

Supplementary Material

Refer to Web version on PubMed Central for supplementary material.

ACKNOWLEDGEMENTS

We thank Johnna R. St. Clair for assistance with the anisotropy measurements.

Funding

This work was supported by NSF grant MCB1715525 (D.P.R) and NIH grant GM122493 (E.L.).

ABBREVIATIONS:

DHE	Dehydroergosterol/ergosta-5,7,9(11),22-tetraen-3β-ol
DLS	dynamic light scattering
DMSO	dimethyl sulfoxide
Fmoc	fluoronylmethoxycarbonyl
FRET	Förster resonance energy transfer
HFIP	hexafluoroisopropanol
hIAPP	human islet amyloid polypeptide
HPLC	high performance liquid chromatography
IAPP	islet amyloid polypeptide
LUV	large unilamellar vesicles
MALDI-TOF	time-of-flight matrix-assisted laser desorption ionization
MLV	multilamellar vesicles
NBD-DOPE	1,2-dioleoyl-sn-glycero-3-phosphoethanolamine-N-(7-nitro-2–1,3-benzoxadiazol-4-yl)
POPC	1-palmitoyl-2-oleoyl-sn-glycero-3-phosphocholine
POPS	1-palmitoyl-2-oleoyl-sn-glycero-3-phospho-L-serine
PS	phosphatidylserine
Rho-DOPE	1,2-dioleoyl-sn-glycero-3-phosphoethanolamine-N-(lissamine rhodamine B sulfonyl)
T2D	type-2 diabetes
T_{50}	the time to reach 50% of the signal change in a thioflavin-T amyloid assay
TEM	transmission electron microscopy
TFA	trifluoroacetic acid.

References:

[1]. Hay DL, Chen S, Lutz TA, Parkes DG, and Roth JD (2015) Amylin: pharmacology, physiology, and clinical potential, Pharmacol Rev 67, 564–600. [PubMed: 26071095]

[2]. Clark A, Cooper GJ, Lewis CE, Morris JF, Willis AC, Reid KB, and Turner RC (1987) Islet amyloid formed from diabetes-associated peptide may be pathogenic in type-2 diabetes, Lancet (London, England) 2, 231–234.

[3]. Cooper GJ, Willis AC, Clark A, Turner RC, Sim RB, and Reid KB (1987) Purification and characterization of a peptide from amyloid-rich pancreases of type 2 diabetic patients, Proc Natl Acad Sci U S A 84, 8628–8632. [PubMed: 3317417]

[4]. Westermark P, Wernstedt C, Wilander E, Hayden DW, O'Brien TD, and Johnson KH (1987) Amyloid fibrils in human insulinoma and islets of Langerhans of the diabetic cat are derived from a neuropeptide-like protein also present in normal islet cells, Proc Natl Acad Sci U S A 84, 3881–3885. [PubMed: 3035556]

[5]. Westermark P, Andersson A, and Westermark GT (2011) Islet amyloid polypeptide, islet amyloid, and diabetes mellitus, Physiol Rev 91, 795–826. [PubMed: 21742788]

[6]. Cao P, Abedini A, and Raleigh DP (2013) Aggregation of islet amyloid polypeptide: from physical chemistry to cell biology, Curr Opin Struct Biol 23, 82–89. [PubMed: 23266002]

[7]. Akter R, Cao P, Noor H, Ridgway Z, Tu L-H, Wang H, Wong AG, Zhang X, Abedini A, Schmidt AM, and Raleigh DP (2016) Islet amyloid polypeptide: structure, function, and pathophysiology, J Diabetes Res 2016, 2798269. [PubMed: 26649319]

[8]. Clark A, Wells CA, Buley ID, Cruickshank JK, Vanhegan RI, Matthews DR, Cooper GJ, Holman RR, and Turner RC (1988) Islet amyloid, increased A-cells, reduced B-cells and exocrine fibrosis: quantitative changes in the pancreas in type 2 diabetes, Diabetes Res 9, 151–159. [PubMed: 3073901]

[9]. de Koning EJ, Bodkin NL, Hansen BC, and Clark A (1993) Diabetes mellitus in Macaca mulatta monkeys is characterised by islet amyloidosis and reduction in beta-cell population, Diabetologia 36, 378–384. [PubMed: 8314440]

[10]. Kahn SE, Andrikopoulos S, and Verchere CB (1999) Islet amyloid: a long-recognized but underappreciated pathological feature of type 2 diabetes, Diabetes 48, 241–253. [PubMed: 10334297]

[11]. Kahn SE, Zraika S, Utzschneider KM, and Hull RL (2009) The beta cell lesion in type 2 diabetes: there has to be a primary functional abnormality, Diabetologia 52, 1003–1012. [PubMed: 19326096]

[12]. Potter KJ, Abedini A, Marek P, Klimek AM, Butterworth S, Driscoll M, Baker R, Nilsson MR, Warnock GL, Oberholzer J, Bertera S, Trucco M, Korbutt GS, Fraser PE, Raleigh DP, and Verchere CB (2010) Islet amyloid deposition limits the viability of human islet grafts but not porcine islet grafts, Proc Natl Acad Sci U S A 107, 4305–4310. [PubMed: 20160085]

[13]. Abedini A, and Schmidt AM (2013) Mechanisms of islet amyloidosis toxicity in type 2 diabetes, FEBS Lett 587, 1119–1127. [PubMed: 23337872]

[14]. Cao P, Marek P, Noor H, Patsalo V, Tu LH, Wang H, Abedini A, and Raleigh DP (2013) Islet amyloid: from fundamental biophysics to mechanisms of cytotoxicity, FEBS Lett 587, 1106–1118. [PubMed: 23380070]

[15]. Mirzabekov TA, Lin MC, and Kagan BL (1996) Pore formation by the cytotoxic islet amyloid peptide amylin, J Biol Chem 271, 1988–1992. [PubMed: 8567648]

[16]. Janson J, Ashley RH, Harrison D, McIntyre S, and Butler PC (1999) The mechanism of islet amyloid polypeptide toxicity is membrane disruption by intermediate-sized toxic amyloid particles, Diabetes 48, 491–498. [PubMed: 10078548]

[17]. Hebda JA, and Miranker AD (2009) The interplay of catalysis and toxicity by amyloid intermediates on lipid bilayers: insights from type II diabetes, Annu Rev Biophys 38, 125–152. [PubMed: 19416063]

[18]. Sparr E, Engel MF, Sakharov DV, Sprong M, Jacobs J, de Kruijff B, Hoppener JW, and Killian JA (2004) Islet amyloid polypeptide-induced membrane leakage involves uptake of lipids by forming amyloid fibers, FEBS Lett 577, 117–120. [PubMed: 15527771]

[19]. Jayasinghe SA, and Langen R (2005) Lipid membranes modulate the structure of islet amyloid polypeptide, Biochemistry 44, 12113–12119. [PubMed: 16142909]

[20]. Engel MF, Khemtemourian L, Kleijer CC, Meeldijk HJ, Jacobs J, Verkleij AJ, de Kruijff B, Killian JA, and Hoppener JW (2008) Membrane damage by human islet amyloid polypeptide through fibril growth at the membrane, Proc Natl Acad Sci U S A 105, 6033–6038. [PubMed: 18408164]

[21]. Engel MF (2009) Membrane permeabilization by islet amyloid polypeptide, Chem Phys Lipids 160, 1–10. [PubMed: 19501206]

[22]. Caillon L, Lequin O, and Khemtemourian L (2013) Evaluation of membrane models and their composition for islet amyloid polypeptide-membrane aggregation, Biochim Biophys Acta 1828, 2091–2098. [PubMed: 23707907]

[23]. Kegulian NC, Sankhagowit S, Apostolidou M, Jayasinghe SA, Malmstadt N, Butler PC, and Langen R (2015) Membrane curvature-sensing and curvature-inducing activity of islet amyloid polypeptide and its implications for membrane disruption, J Biol Chem 290, 25782–25793. [PubMed: 26283787]

[24]. Brunham LR, Kruit JK, Verchere CB, and Hayden MR (2008) Cholesterol in islet dysfunction and type 2 diabetes, The Journal of Clinical Investigation 118, 403–408. [PubMed: 18246189]

[25]. Caillon L, Duma L, Lequin O, and Khemtemourian L (2014) Cholesterol modulates the interaction of the islet amyloid polypeptide with membranes, Mol Membr Biol 31, 239–249. [PubMed: 25495656]

[26]. Cho WJ, Trikha S, and Jeremic AM (2009) Cholesterol regulates assembly of human islet amyloid polypeptide on model membranes, J Mol Biol 393, 765–775. [PubMed: 19720065]

[27]. Li Y, Guan LP, Lu T, Li HC, Li ZQ, and Li F (2016) Interactions of the N-terminal domain of human islet amyloid polypeptide with lipid membranes: the effect of cholesterol, Rsc Advances 6, 96837–96846.

[28]. McHenry AJ, Brender JR, Hartman K, and Ramamoorthy A (2011) Lipid composition and raft domain formation on the IAPP-membrane interaction: the tole of cholesterol on the inhibition of IAPP (amylin) fibrilization and the reduction of membrane disruption in model liposomes and mouse pancreatic islets, Biophysical Journal 100, 541–541.

[29]. Singh S, Trikha S, Bhowmick DC, Sarkar AA, and Jeremic AM (2015) Role of cholesterol and phospholipids in amylin misfolding, aggregation and etiology of islet amyloidosis, Adv Exp Med Biol 855, 95–116. [PubMed: 26149927]

[30]. Sciacca, Michele FM, Lolicato F, Di Mauro G, Milardi D, D'Urso L, Satriano C, Ramamoorthy A, and La Rosa C (2016) The role of cholesterol in driving IAPP-membrane interactions, Biophysical Journal 111, 140–151. [PubMed: 27410742]

[31]. Trikha S, and Jeremic AM (2011) Clustering and internalization of toxic amylin oligomers in pancreatic cells require plasma membrane cholesterol, J Biol Chem 286, 36086–36097. [PubMed: 21865171]

[32]. Xu X, and London E (2000) The effect of sterol structure on membrane lipid domains reveals how cholesterol can induce lipid domain formation, Biochemistry 39, 843–849. [PubMed: 10653627]

[33]. Bakht O, Pathak P, and London E (2007) Effect of the structure of lipids favoring disordered domain formation on the stability of cholesterol-containing ordered domains (lipid rafts): Identification of multiple raft-stabilization mechanisms, Biophysical Journal 93, 4307–4318. [PubMed: 17766350]

[34]. Grouleff J, Irudayam SJ, Skeby KK, and Schiott B (2015) The influence of cholesterol on membrane protein structure, function, and dynamics studied by molecular dynamics simulations, Biochim Biophys Acta 1848, 1783–1795. [PubMed: 25839353]

[35]. Daffu G, Shen X, Senatus L, Thiagarajan D, Abedini A, Hurtado Del Pozo C, Rosario R, Song F, Friedman RA, Ramasamy R, and Schmidt AM (2015) RAGE suppresses ABCG1-mediated macrophage cholesterol efflux in diabetes, Diabetes 64, 4046–4060. [PubMed: 26253613]

[36]. Maxfield FR, and Tabas I (2005) Role of cholesterol and lipid organization in disease, Nature 438, 612–621. [PubMed: 16319881]

[37]. Zhang X, St Clair JR, London E, and Raleigh DP (2017) Islet amyloid polypeptide membrane interactions: effects of membrane composition, Biochemistry 56, 376–390. [PubMed: 28054763]

[38]. Middleton ER, and Rhoades E (2010) Effects of curvature and composition on α-synuclein binding to lipid vesicles, Biophysical Journal 99, 2279–2288. [PubMed: 20923663]

[39]. Xu W, Wei G, Su H, Nordenskiold L, and Mu Y (2011) Effects of cholesterol on pore formation in lipid bilayers induced by human islet amyloid polypeptide fragments: a coarse-grained molecular dynamics study, Physical review. E, Statistical, nonlinear, and soft matter physics 84, 051922.

[40]. Dies H, Toppozini L, and Rheinstadter MC (2014) The interaction between amyloid-beta peptides and anionic lipid membranes containing cholesterol and melatonin, PLoS One 9, e99124. [PubMed: 24915524]

[41]. Sasahara K, Morigaki K, and Shinya K (2014) Amyloid aggregation and deposition of human islet amyloid polypeptide at membrane interfaces, The FEBS journal 281, 2597–2612. [PubMed: 24702784]

[42]. Seghezza S, Diaspro A, Canale C, and Dante S (2014) Cholesterol drives abeta(1–42) interaction with lipid rafts in model membranes, Langmuir 30, 13934–13941. [PubMed: 25360827]

[43]. Yu X, and Zheng J (2012) Cholesterol promotes the interaction of alzheimer β-amyloid monomer with lipid bilayer, J Mol Biol 421, 561–571. [PubMed: 22108168]

[44]. Di Scala C, Yahi N, Lelièvre C, Garmy N, Chahinian H, and Fantini J (2013) Biochemical identification of a linear cholesterol-binding domain within alzheimer's β amyloid peptide, ACS Chemical Neuroscience 4, 509–517. [PubMed: 23509984]

[45]. Di Scala C, Chahinian H, Yahi N, Garmy N, and Fantini J (2014) Interaction of alzheimer's β-amyloid peptides with cholesterol: mechanistic insights into amyloid pore formation, Biochemistry 53, 4489–4502. [PubMed: 25000142]

[46]. Zhao LN, Chiu S-W, Benoit J, Chew LY, and Mu Y (2011) Amyloid β peptides aggregation in a mixed membrane bilayer: a molecular dynamics study, The Journal of Physical Chemistry B 115, 12247–12256. [PubMed: 21910473]

[47]. Abedini A, and Raleigh DP (2005) Incorporation of pseudoproline derivatives allows the facile synthesis of human IAPP, a highly amyloidogenic and aggregation-prone polypeptide, Org Lett 7, 693–696. [PubMed: 15704927]

[48]. Marek P, Woys AM, Sutton K, Zanni MT, and Raleigh DP (2010) Efficient microwave-assisted synthesis of human islet amyloid polypeptide designed to facilitate the specific incorporation of labeled amino acids, Org Lett 12, 4848–4851. [PubMed: 20931985]

[49]. Abedini A, Singh G, and Raleigh DP (2006) Recovery and purification of highly aggregation-prone disulfide-containing peptides: application to islet amyloid polypeptide, Anal Biochem 351, 181–186. [PubMed: 16406209]

[50]. Nilsson MR, and Raleigh DP (1999) Analysis of amylin cleavage products provides new insights into the amyloidogenic region of human amylin, J Mol Biol 294, 1375–1385. [PubMed: 10600392]

[51]. Nilsson MR, Driscoll M, and Raleigh DP (2002) Low levels of asparagine deamidation can have a dramatic effect on aggregation of amyloidogenic peptides: implications for the study of amyloid formation, Protein Sci 11, 342–349. [PubMed: 11790844]

[52]. Dunkelberger EB, Buchanan LE, Marek P, Cao P, Raleigh DP, and Zanni MT (2012) Deamidation accelerates amyloid formation and alters amylin fiber structure, J Am Chem Soc 134, 12658–12667. [PubMed: 22734583]

[53]. Stewart JC (1980) Colorimetric determination of phospholipids with ammonium ferrothiocyanate, Anal Biochem 104, 10–14. [PubMed: 6892980]

[54]. Cao P, Abedini A, Wang H, Tu LH, Zhang X, Schmidt AM, and Raleigh DP (2013) Islet amyloid polypeptide toxicity and membrane interactions, Proc Natl Acad Sci U S A 110, 19279–19284. [PubMed: 24218607]

[55]. Last NB, Rhoades E, and Miranker AD (2011) Islet amyloid polypeptide demonstrates a persistent capacity to disrupt membrane integrity, Proc Natl Acad Sci U S A 108, 9460–9465. [PubMed: 21606325]

[56]. Lentz BR (1993) Use of fluorescent probes to monitor molecular order and motions within liposome bilayers, Chem Phys Lipids 64, 99–116. [PubMed: 8242843]

[57]. Wenz JJ, and Barrantes FJ (2003) Steroid structural requirements for stabilizing or disrupting lipid domains, Biochemistry 42, 14267–14276. [PubMed: 14640695]

[58]. Wang JW, Megha, and London E (2004) Relationship between sterol/steroid structure and participation in ordered lipid domains (lipid rafts): Implications for lipid raft structure and function, Biochemistry 43, 1010–1018. [PubMed: 14744146]

[59]. Megha,Bakht O, and London E (2006) Cholesterol precursors stabilize ordinary and ceramide-rich ordered lipid domains (lipid rafts) to different degrees. Implications for the Bloch hypothesis and sterol biosynthesis disorders, J Biol Chem 281, 21903–21913. [PubMed: 16735517]

[60]. Wong AG, Wu C, Hannaberry E, Watson MD, Shea JE, and Raleigh DP (2016) Analysis of the amyloidogenic potential of pufferfish (takifugu rubripes) islet amyloid polypeptide highlights the limitations of thioflavin-T assays and the difficulties in defining amyloidogenicity, Biochemistry 55, 510–518. [PubMed: 26694855]

[61]. Weise K, Radovan D, Gohlke A, Opitz N, and Winter R (2010) Interaction of hIAPP with model raft membranes and pancreatic β-cells: cytotoxicity of hIAPP oligomers, ChemBioChem 11, 1280–1290. [PubMed: 20440729]

[62]. Yang ST, Kiessling V, Simmons JA, White JM, and Tamm LK (2015) HIV gp41-mediated membrane fusion occurs at edges of cholesterol-rich lipid domains, Nature Chemical Biology 11, 424. [PubMed: 25915200]

[63]. Yang ST, Kiessling V, and Tamm LK (2016) Line tension at lipid phase boundaries as driving force for HIV fusion peptide-mediated fusion, Nature Communications 7, 11401.

[64]. Yang ST, Kreutzberger AJB, Kiessling V, Ganser-Pornillos BK, White JM, and Tamm LK (2017) HIV virions sense plasma membrane heterogeneity for cell entry, Sci Adv 3, e1700338. [PubMed: 28782011]

[65]. Pathak P, and London E (2011) Measurement of lipid nanodomain (raft) formation and size in sphingomyelin/POPC/cholesterol vesicles shows TX-100 and transmembrane helices increase domain size by coalescing preexisting nanodomains but do not induce domain formation, Biophys J 101, 2417–2425. [PubMed: 22098740]

[66]. Fantini J, and Yahi N (2010) Molecular insights into amyloid regulation by membrane cholesterol and sphingolipids: common mechanisms in neurodegenerative diseases, Expert Rev Mol Med 12, e27. [PubMed: 20807455]

[67]. Ke PC, Sani MA, Ding F, Kakinen A, Javed I, Separovic F, Davis TP, and Mezzenga R (2017) Implications of peptide assemblies in amyloid diseases, Chem Soc Rev 46, 6492–6531. [PubMed: 28702523]

[68]. Brown AM, and Bevan DR (2017) Influence of sequence and lipid type on membrane perturbation by human and rat amyloid beta-peptide (1–42), Archives of Biochemistry and Biophysics 614, 1–13. [PubMed: 27884599]

[69]. Kirsch C, Eckert GP, and Mueller WE (2002) Cholesterol attenuates the membrane perturbing properties of beta-amyloid peptides, Amyloid 9, 149–159. [PubMed: 12408677]

[70]. Sani MA, Gehman JD, and Separovic F (2011) Lipid matrix plays a role in Abeta fibril kinetics and morphology, FEBS Lett 585, 749–754. [PubMed: 21320494]

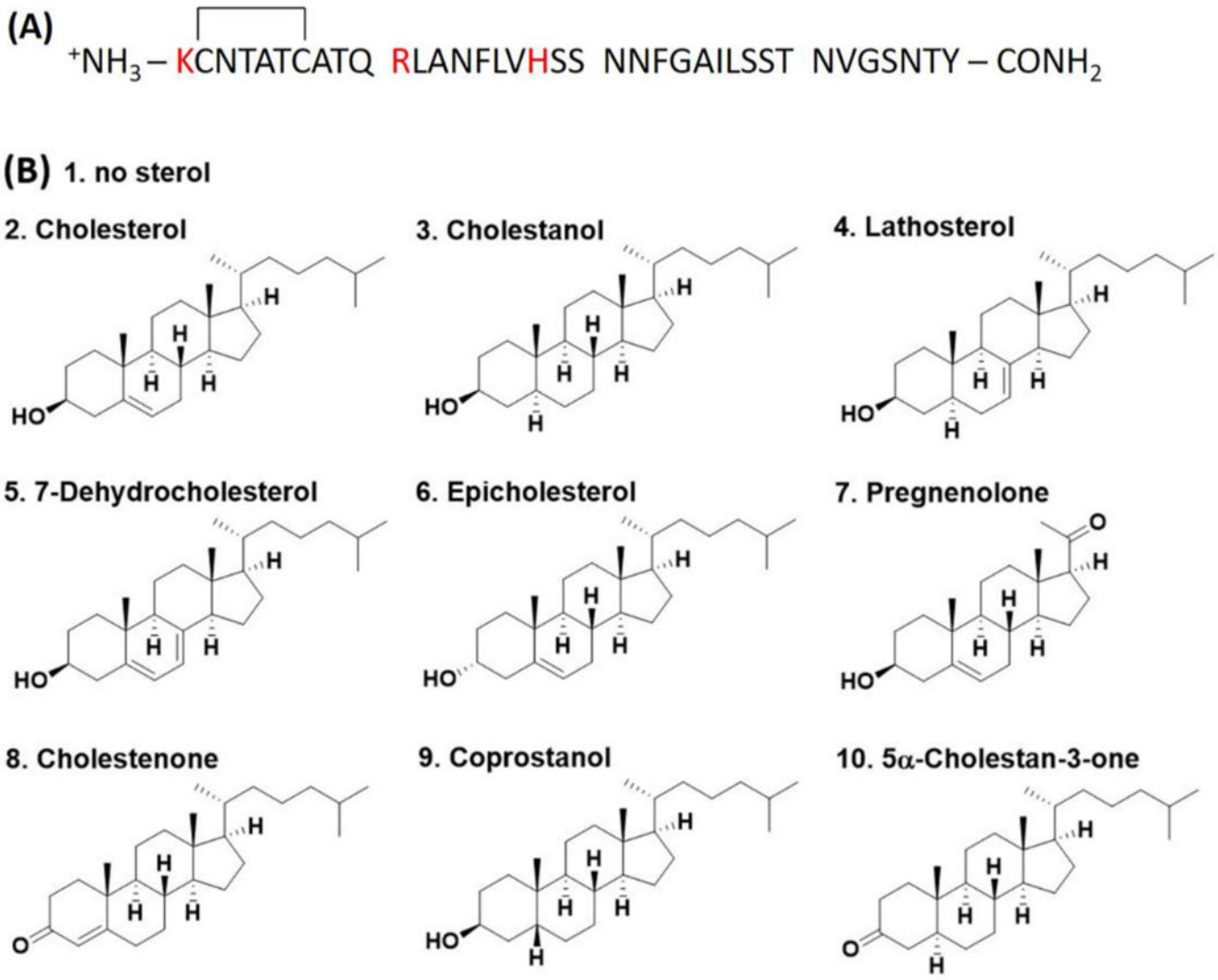

Figure 1. Molecules studied.

(A) The sequence of human IAPP. The peptide has an amidated C-terminus and contains a disulfide bridge between residues 2 and 7. Residues which have the potential to be positively charged near physiological pH are colored red. **(B) Structures of the different sterols studied.** The numbering is used throughout the remaining figures to denote the different sterols.

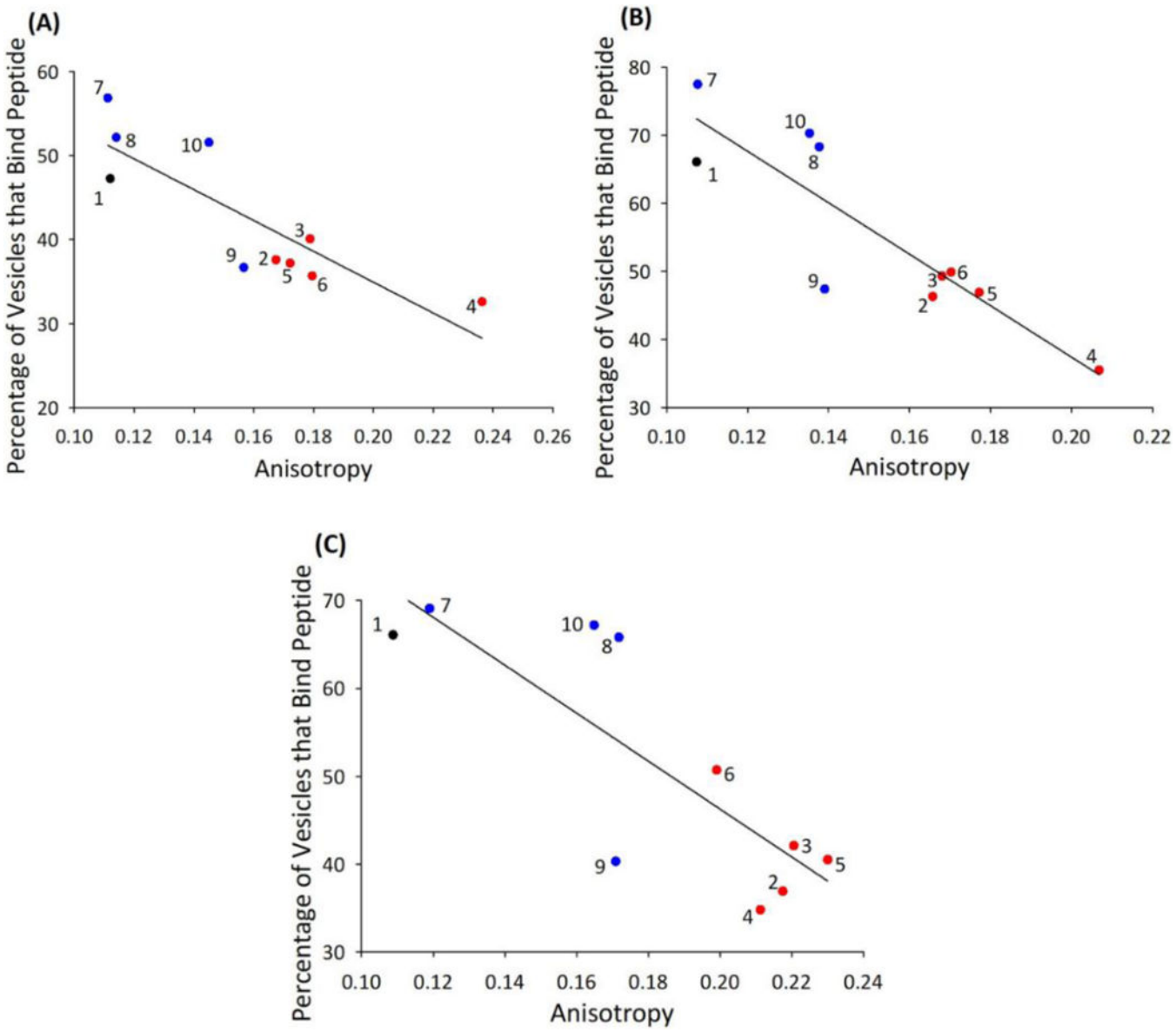

Figure 2. Correlation between the percentage of vesicles that bind peptide and the effect of different sterols on membrane order.

The percentage of LUVs that bind hIAPP are plotted against the DPH anisotropy values. LUVs contain **(A)** 20 mol% sterol, 80 mol% POPC. R^2 =0.7219, P-value = 0.0019. **(B)** 20 mol% sterol, 10 mol% POPS and 70 mol% POPC. R^2 =0.7719, P-value = 0.0008. **(C)** 40 mol% sterol, 10 mol% POPS and 50 mol% POPC. R^2 =0.6637, P-value = 0.0041. The sterol numbering corresponds to that shown in table-1 and figure-1. Samples with sterols/ compositions that do not promote tight lipid packing are in blue. Samples with sterols that do promote tight lipid packing are in red. Note that corresponding samples without sterol also included (black point). The POPS mole% is the same for samples in the presence and in the absence of sterols.

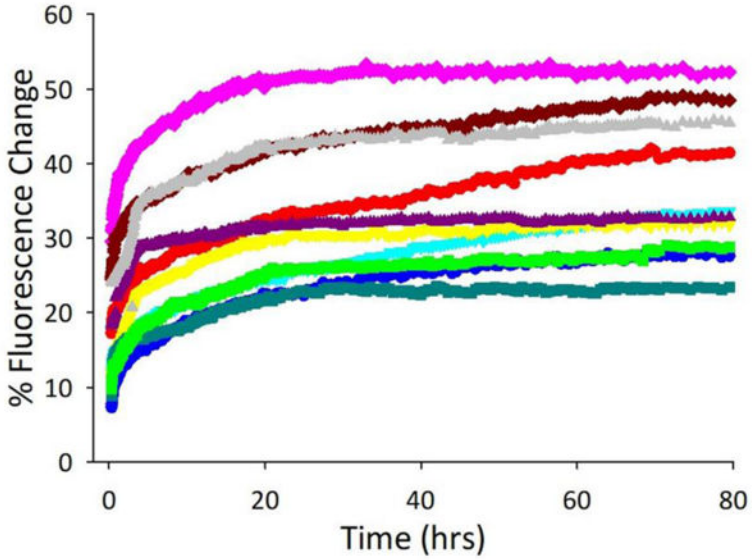

Figure 3. Effect of different sterols on membrane leakage.

The time course of carboxyfluorescein leakage experiments are displayed for vesicles containing 100 mol% POPC (red), 80 mol% POPC and 20 mol% sterol: cholesterol (blue), cholestanol (cyan), lathosterol (dark cyan), 7-dehydrocholesterol (yellow), epicholesterol (green), pregnenolone (pink), cholestenone (dark red), coprostanol (purple) and 5α-cholestan-3 one (grey). Experiments were conducted in 20 mM Tris·HCl, 100 mM NaCl, pH 7.4 at 25 °C with 400 μM lipid and 20 μM hIAPP.

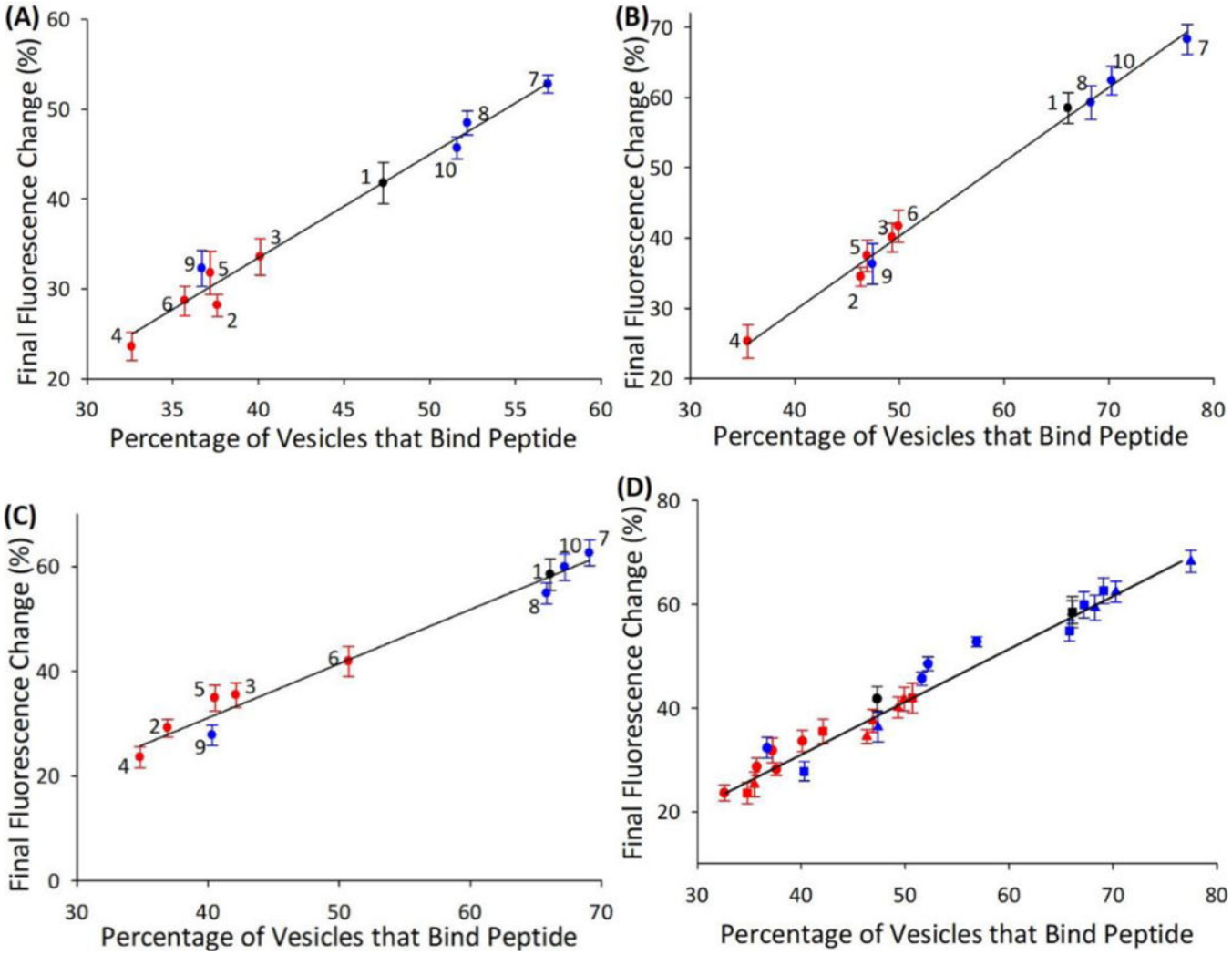

Figure 4. Correlation between the percentage of vesicles that bind peptide and the percent leakage.

The final carboxyfluorescein fluorescence change is plotted vs the fraction of vesicles that bind peptide as deduced from sucrose gradient experiments. LUVs contain **(A)** 20 mol% sterol, 80 mol% POPC. R^2 =0.9772, P-value = 0.0001. **(B)** 20 mol% sterol, 10 mol% POPS and 70 mol% POPC. R^2 =0.9941, P-value = 0.0001. **(C)** 40 mol% sterol, 10 mol% POPS and 50 mol% POPC. R^2 =0.9766, P-value = 0.0001. **(D)** All lipid compositions. R^2 =0.9700, P-value = 0.0001. Note that corresponding samples without sterol are also included. The sterol numbering in (A) to (C) corresponds to that shown in table-1 and figure-1.

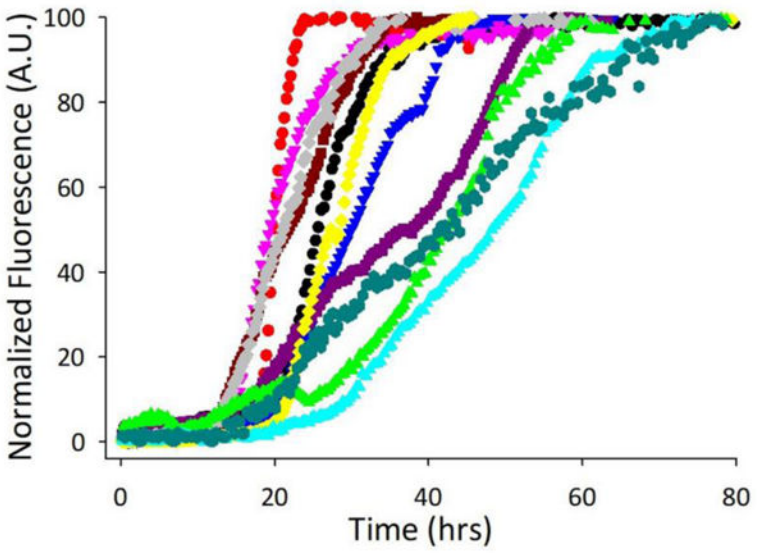

Figure 5. Effect of different sterols upon amyloid formation.

Vesicles were prepared with different sterols and the zwitterionic lipid POPC. The results of thioflavin-T assays are displayed. Data are plotted for hIAPP in solution (black), LUVs containing 100 mol% POPC (red) or LUVs containing 80 mol% POPC and 20 mol% of the following sterols: cholesterol (blue), cholestanol (cyan), lathosterol (dark cyan), 7-dehydrocholesterol (yellow), epicholesterol (green), pregnenolone (pink), cholestenone (dark red), coprostanol (purple) and 5α-cholestan-3 one (grey). Experiments were conducted in 20 mM Tris·HCl, 100 mM NaCl, pH 7.4 at 25 °C with 400 μM lipid and 20 μM hIAPP.

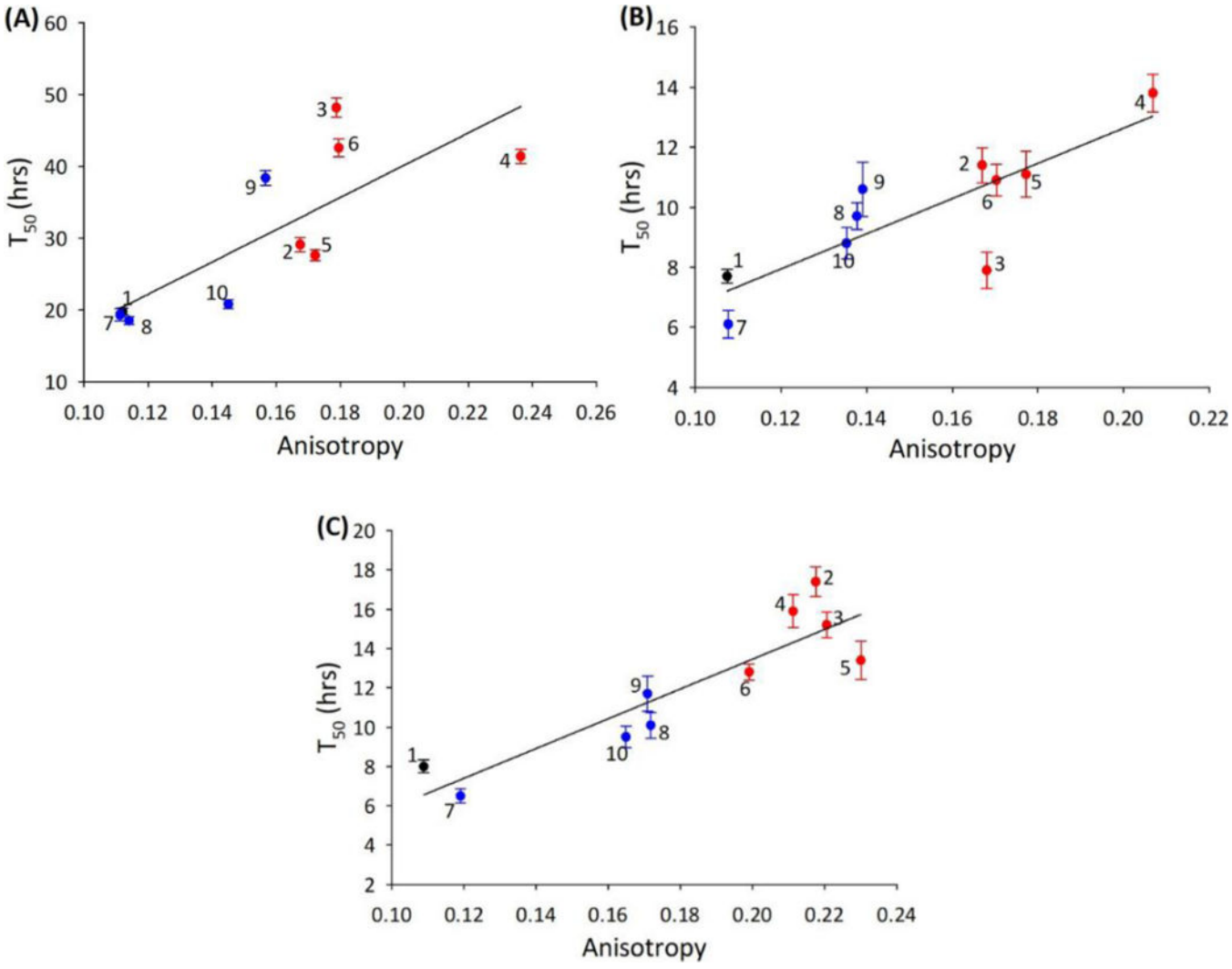

Figure 6. Correlation between the time required to form amyloid and the effect of different sterols on membrane order.

The values of T_{50} for amyloid formation are plotted against the LUV anisotropy values. LUVs contain **(A)** 20 mol% sterol, 80 mol% POPC. R^2 =0.6125, P-value = 0.0072. **(B)** 20 mol% sterol, 10 mol% POPS and 70 mol% POPC. R^2 =0.6946, P-value = 0.0027. **(C)** 40 mol% sterol, 10 mol% POPS and 50 mol% POPC. R^2 =0.8117, P-value = 0.0004. The numbering corresponds to that shown in table-1 and figure-1. Note that corresponding samples without sterol are also included.

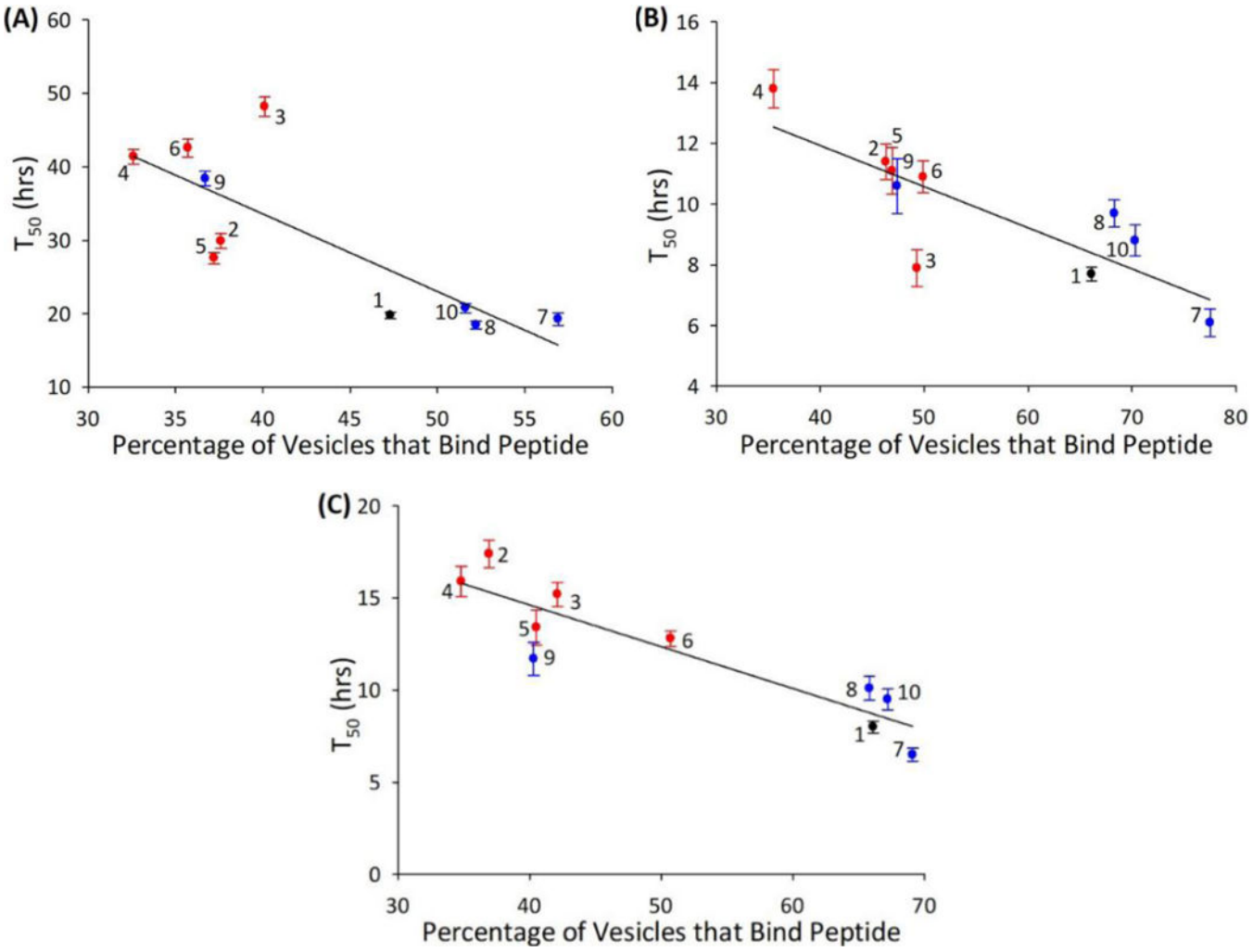

Figure 7. Correlation between the time required to form amyloid and the percentage of vesicles that bind peptide.

The values of T_{50} for amyloid formation are plotted against the percentage of vesicles that binding peptide. LUVs contain **(A)** 20 mol% sterol, 80 mol% POPC. R^2 =0.6347, P-value = 0.0058. **(B)** 20 mol% sterol, 10 mol% POPS and 70 mol% POPC. R^2 =0.6843, P-value = 0.0031. **(C)** 40 mol% sterol, 10 mol% POPS and 50 mol% POPC. R^2 =0.8161, P-value = 0.0003. The sterol numbering corresponds to that shown in table-1 and figure-1. Note that corresponding samples without sterol are also included.

Table 1.

Anisotropy values for LUVs containing different amounts of POPC, POPS and various sterols.

Experiments were conducted in 20 mM Tris·HCl, 100 mM NaCl, pH 7.4 at 25 °C with 400 μM lipid.

		DPH Fluorescence Anisotropy		
		Lipid Composition		
	Sterol	**POPC with 20% sterol, no PS**	**POPC with 20% sterol, 10% PS**	**POPC with 40% sterol, 10%PS**
1	no sterol	0.112±0.0055	0.107±0.0031	0.109±0.0018
2	Cholesterol	0.167±0.0069	0.166±0.0056	0.218±0.0074
3	Cholestanol	0.179±0.0122	0.168±0.0051	0.221±0.0054
4	Lathosterol	0.236±0.0055	0.207±0.0069	0.211±0.0037
5	7-Dehydrocholesterol	0.172±0.0072	0.177±0.0034	0.230±0.0077
6	Epicholesterol	0.180±0.0074	0.170±0.0024	0.199±0.0057
7	Pregnenolone	0.111±0.0062	0.108±0.0018	0.119±0.0043
8	Cholestenone	0.114±0.0055	0.138±0.0035	0.172±0.0053
9	Coprostanol	0.157±0.0064	0.139±0.0042	0.171±0.0044
10	5α-cholestan-3-one	0.145±0.0079	0.135±0.0037	0.165±0.0038

Table 2.

Percentage of vesicles that bind peptide for vesicles containing different amounts of POPC, POPS and various sterols.

Experiments were conducted in 20 mM Tris·HCl, 100 mM NaCl, pH 7.4 at 25 °C with 400 μM lipid and 20 μM hIAPP.

		Percentage of Vesicles Binding Peptide		
		Lipid Composition		
	Sterol	**POPC with 20% sterol, no POPS**	**POPC with 20% sterol, 10% POPS**	**POPC with 40% sterol, 10% POPS**
1	no sterol	47.3	66.1	66.1
2	Cholesterol	37.6	46.3	36.9
3	Cholestanol	40.1	49.3	42.1
4	Lathosterol	32.6	35.5	34.8
5	7-Dehydrocholesterol	37.2	46.9	40.5
6	Epicholesterol	35.7	49.9	50.7
7	Pregnenolone	56.9	77.5	69.1
8	Cholestenone	52.2	68.3	65.8
9	Coprostanol	36.7	47.4	40.3
10	5α-cholestan-3-one	51.6	70.3	67.2